Review of design based on AASHTO LRFD Seismic—Design in the transverse direction is carried out for each bent independently (stand-alone design). In the longitudinal direction, the bents were considered linked by the superstructure. In both cases any participation of the abutments was ignored. For a detailed review of this design, the readers are directed to Caltrans (2006b).

Design began by assuming the columns are reinforced with 26D44 (#14) bars and a D25 (#8) spiral spaced at 125 mm (5 in.). Next, it was checked that the bridge complies with the balanced mass and stiffness criteria given by AASHTO LRFD Seismic and a preliminary capacity-demand assessment was conducted. In order to do so, moment-curvature analyses were performed to determine the yield moment, yield curvature and ultimate curvature and cracked section moment of inertia of the column sections. The ultimate curvature was found at a concrete strain equal 0.018.

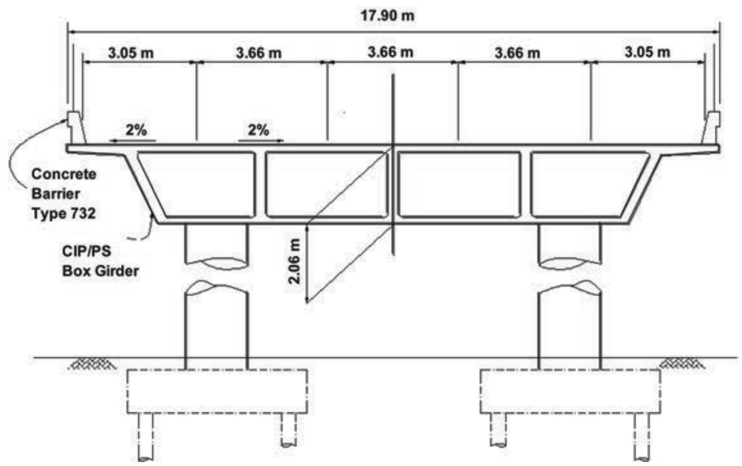

Fig. 7—Superstructure section and interior bent, trial design CA-1.

Then, using the plastic hinge method, the yield displacement and displacement capacity (to reach concrete strain equal 0.018) of each bent was estimated. For bent 2, Δ_y = 184 mm (7.24 in.) and Δ_c = 908 mm (35.75 in.) and for bent 3, Δ_y = 210 mm (8.27 in.) and Δ_c = 1026 mm (40.39 in.). These values are valid for transverse and longitudinal response. The ductility capacity of these bents is close to 5 exceeds the minimum 3 specified in AASHTO LRFD Seismic.

Next, displacement demand was computed in the transverse direction of the bridge. Each bent was treated separately; the mass that was used corresponded to the weight supported by each bent. These calculations resulted in displacement demands of 478 mm and 524 mm (18.82 in. and 20.63 in.) for bents 2 and 3 respectively. The ductility demand is 2.6 and 2.5 for bents 2 and 3 respectively. These values are significantly less than the ductility capacity and less than maximum ductility allowed by AASHTO LRFD Seismic. Therefore, it was concluded that the sections satisfied the minimum design requirements and design was continued with more detailed analyses.

Pushover analyses were then used to get a best estimate of the displacement capacity and stiffness of the bents in the transverse and longitudinal directions of the bridge, now accounting for the flexibility of the integral cap-beam and considering that the columns are partially embedded in soil. In the transverse direction, Δ_c = 882 mm (34.72 in.) and Δ_D= 564 mm (22.20 in.) for bent 2. For bent 3, Δ_C = 988 mm (38.90 in.) and Δ_D= 601 mm (23.66 in.). A P-Δ check showed that the stability index was close to 25%. Since 25% is the limit allowed in AASHTO LRFD Seismic, it was concluded that the assumed reinforcement was appropriate and that design was controlled by P-Δ effects rather than by displacement capacity.

The pushover analysis in the longitudinal direction considered all columns in the bridge lumped together and all the mass of the bridge. The participation of the abutments was neglected. In the longitudinal direction, Δ_c = 947 mm (37.28 in.) for bent two and Δ_c = 1063 mm (41.85 in.) for bent three. The displacement demand was 599 mm (23.58 in.) for the two bents since the superstructure acts as a rigid link between them. The ductility demand is 3.11 for bent two and 2.76 for bent three. Since the induced P-Δ moments are 24% of the flexural capacity of the columns the longitudinal design was also controlled by P-Δ effects and the chosen reinforcement was considered appropriate.

Finally, a shear demand-capacity check was performed for the columns. The shear demand was based on the over-strength flexural capacity of the columns, the integral cap-beams were designed and seismic forces developed in the superstructure due to longitudinal displacement of the bridge were determined.

Direct Displacement-Based Design—This design is based on the geometry, configuration, materials and section properties as reported at the beginning of the design example. Transverse and longitudinal responses are considered.

Design Objective—Under the design earthquake represented by the displacement spectra described previously, the bridge shall reach one or more of the following limits: damage-control strains in the columns, stability index equal to 25%.

Assessment of Target Displacement—According to the AASHTO LRFD Seismic design report, the reinforced concrete in the bents has the following properties: f'_{ce} = 36 MPa (5,250 psi), f_{ye} = 455 MPa (66 ksi), ε_y = 455/200000 = 0.0022, ε_{su} = 0.1, f_{yh} = 414 MPa (60 ksi). Complying with minimum reinforcement and spacing requirements, D44 (#14) longitudinal bars and a D25 (#8) spiral spaced 130 mm (5.1 in) are chosen for the columns.

Table 2—Target displacements Trial design CA-1

	H m (ft)	D m (ft)	P kN (kip)	Δ_y mm (in)	Δ_{DC} mm (in)	$\Delta_{\theta s}$ mm (in)
Bent 2	13.4 (44.0)	1.83 (6)	6714 (1509)	178 (7.01)	805 (31.69)	640 (25.2)
Bent 3	14.3 (46.90)	1.83 (6)	6557 (1474)	202 (7.95)	903 (35.55)	650 (25.6)

For the given amount of shear and confinement reinforcement, the damage control concrete strain computed with Eq. 18 is 0.014, this is less than the limit strain used in the AASHTO LRFD Seismic design for a life-safety limit state. The damage control displacement of the bents is determined with the plastic hinge method, assuming single bending in the columns. These calculations are valid for the two directions of design. The Yield displacement Δ_y and damage-control displacement Δ_{DC} are shown in Table 2, along with the stability–based displacement (Eq. 19-20) and some parameters used in their calculation. It is observed in this table that *P*-Δ based displacement controls design and becomes the target design displacement. The bents are skewed 20 degrees, however since the target displacement and other response parameters are the same in the in-plane and out-of-plane direction of the bent, these are also the same in the transverse and longitudinal directions of the bridge (Eq. 21-22).

Strength Distribution—The application of DDBD results in the total strength *V*, required in each design direction, to meet performance specified in the design objective. The strength of seat-type abutments V_a is generally known or can be estimated before design. The contribution of the abutments to the total strength of the bridge is given by Eq. 23. Therefore, satisfying equilibrium of forces, the contribution of the piers to the strength of the bridge is given by Eq. 24.

$$v_a = \frac{V_a}{V} \tag{23}$$

$$v_p = 1 - v_a \tag{24}$$

Since it is likely that all piers develop their strength and perform inelastically during the earthquake, it is possible to distribute strength among piers such that all piers require the same reinforcement ratio (Priestley et al. 2007). Assuming that bent columns with the same reinforcement ratio have the same ratio of cracked to gross inertia, Eq. 25 gives the ratio of total strength v_i taken by bent *i*, with *n* columns of diameter D_i, shear height H_{si} and ductility μ_i, required to satisfy force equilibrium. In this trial design, since the columns are pinned at the base, H_s equals the height of the columns (Suarez 2008).

$$v_i = (1 - v_a)\frac{\dfrac{n_i \mu_i D_i^3}{H_{si}}}{\sum \dfrac{n_i \mu_i D_i^3}{H_{si}}} \qquad \mu_i \le 1 \tag{25}$$

Recognizing that even if the abutments are not designed as part of the earthquake resisting system they can have some effect on the performance of the bridge. As a starting point, it is assumed that the abutments will take 10% of the total seismic forces in the transverse and longitudinal directions.

Design in Transverse Direction—The design in the transverse direction will account for interaction between the superstructure, bents and abutments. The superstructure section, shown in Fig. 7, has an out-of-plane inertia I = 222 m^4 (25,695 ft^4), an elastic modulus E_s = 26,500 MPa (3713 ksi), and a weight W_s = 260 kN/m (17.82 kip/ft). The abutments are assumed to have an elasto-plastic response. The transverse strength or yield force for the abutments is computed considering sacrificial shear keys that will break during the design earthquake. The residual strength in the abutment comes from friction between the superstructure and the abutment. Assuming a friction coefficient of 0.2, with a normal force equal to the tributary superstructure weight carried by the abutments, the transverse strength of the abutments is 1300 kN (292 kip). It is assumed that the yield displacement is 50 mm (2 in).

Since the bridge is regular and the superstructure is stiff, the abutments are not expected to restrain the displacement of the super-structure and a RBT profile will be used. The amplitude of the target displacement profile is given by the bent with the least target displacement so Δ_{sys} = 640 mm (25.2 in.). The effective mass comes from the mass of the superstructure, integral bent-caps and one third of the weight of the columns, M_{eff} = 3808 t (21.75 kip s^2/in.).

The ductility at target displacement level is μ_1 = 12.80, μ_2 = 3.59, μ_3 = 3.16, μ_4 = 12.80 (reference for then subindexes is given in Fig. 6). Equivalent damping is computed and combined resulting in ξ_{sys} = 14.4%. Combination of damping is done in terms of work done by each element (Priestley et al 2007).

The level of damping in the bridge results in a displacement demand reduction factor R_ξ = 0.65 and the required period is T_{eff} = 4.1 s (Eq. 14). Finally, the required strength for the bridge in the transverse direction is V = 5700 kN (1276.8 kip) (Eq. 16). At the target displacement, both abutments develop their strength V_a = 2600 kN (582 kip) and υ_a = 45% (Eq. 23). This is 4.5 times the value assumed at the beginning of the process; therefore ξ_{sys} must be re-evaluated to obtain a new V. After a few iterations V = 6447 kN (1444.3 kip) and the participation of the abutments is 39%, as shown in Table 3.

It is important to note that iteration was required since it was chosen to consider the strength of the abutments. Accounting for the strength of the abutments has significantly reduced the demand on the piers.

Table 3—Transverse Design: CA-1

Iteration	Δ_{sys} mm (in)	ξ_{sys}	T_{eff} (s)	V kN (kip)	(V1+V4)/V
1	640 (25.2)	14.4	>Tc	5879.8 (1317.1)	0.1
2	640 (25.2)	13.3	3.9	6313.3 (1414.2)	0.45
3	640 (25.2)	13.1	3.87	6417.2 (1437.5)	0.38
4	640 (25.2)	13	3.86	6447.8 (1444.3)	0.39

Table 4—Longitudinal Design parameters: Trial design CA-1

Iteration	Δ_{sys} mm (in)	ξ_{sys}	T_{eff} (s)	V kN (kip)	(V1+V4)/V
1	640 (25.2)	14.5	>Tc	5699.9 (1276.8)	0.1
2	640 (25.2)	11	3.69	7247.1 (1623.4)	0.8
3	640 (25.2)	10.8	3.66	7349.5 (1646.3)	0.84
4	640 (25.2)	10.9	3.67	7316 (1638.8)	0.82

Design in Longitudinal Direction—The design process along the longitudinal direction is similar to design in transverse direction. Since the columns are pinned to the foundation and they are integral with the superstructure, the target displacement in the longitudinal direction is the same as the capacity in the transverse direction. Also, since the superstructure is stiff and continuous, the displacement at the location of the bents and abutments are constrained to be the same. Therefore, Δ_{sys} and M_{eff} are the same as in transverse direction.

As in the transverse design case, abutments were considered to provide strength to the bridge. Since the longitudinal direction the abutments are designed with knock-off walls, their strength comes from soil mobilization behind the wall pushed by the superstructure. In the AASHTO LRFD Seismic report, the soil passive strength was 6058 kN (1357 kip) at a yield displacement of 76 mm (3 in.) .

Table 4 summarizes the values of the main design parameters during longitudinal design. A few iterations were required as it was found that the abutments contribute with as much as 82% of the total strength in this direction. After four iterations the solution converges, V = 7316 kN (1638.8 kip) and the contribution of the abutments is 82%.

Element Design—In DDBD, the flexural reinforcement is designed using moment-curvature analysis to provide the required strength at a level of curvature compatible with the ductility demand in the element. Table 5 shows the design moments in the transverse M_t and longitudinal direction M_l that resulted from DDBD. These values are followed by P-Δ moments and stability indexes. If the stability index is larger than 8%, the design moment must be increased adding 50% of the P-Δ moment to account for strength reduction caused by P-Δ effects (Priestley et al 2007). The increased moments are then combined using the 100%-30% rule to get the design moment M_E.

Table 5—Bent design. Trial design CA-1

BENT	MT kN.m (kip.ft)	ML kN.m (kip.ft)	MT P-Δ kN.m (kip.ft)	ML P-Δ kN.m (kip.ft)	θ_{sT}	θ_{sL}	ME kN.m kip.ft	ρ (%)	S D/C ratio
2	14975 (11002)	4446 (3266)	4408 (3238)	4408 (3238)	0.29	0.29	17238 (12665)	1.1	0.24
3	14975 (11002)	4446 (3266)	4304 (3162)	4304 (3162)	0.29	0.29	17238 (12665)	1.1	0.25

At the design displacements, the strain in the concrete reaches values of 0.011 for bent 2 and 0.010 for bent 3. These design strains are computed using the plastic hinge method. By section analysis at the design strains, it is found that all columns in the bridge require 20D44 bars as flexural reinforcement, which is a 1.1% steel ratio. Finally, using the modified UCSD shear model (Priestley and Kowalsky 2000), the shear capacity of the section is computed and compared to shear demand at flexural over-strength. The shear demand/capacity ratios are shown in Table 5.

Table 6—Summary of LDFD-Seismic and DDBD designs

LRFD-Seismic							
BENT	Δ_{Ct} (mm)	Δ_{Cl} (mm)	Δ_{Dt} (mm)	Δ_{Dl} (mm)	ρ (%)	Rebar	Spiral
2	882	947	564	599	1.5	26D44	D25@125
3	988	1063	601	599	1.5	26D44	D25@125
DDBD							
BENT	Δ_{Ct} (mm)	Δ_{Cl} (mm)	Δ_{Dt} (mm)	Δ_{Dl} (mm)	ρ (%)	Rebar	Spiral
2	640	640	640	640	1.1	18D44	D25@125
3	640	640	640	640	1.1	18D44	D25@125

Analysis and Comparison—A summary of results of the two designs for this bridge is presented in Table 6. It is observed that accounting by the strength of the abutments in DDBD lead to a reduction in the amount of reinforcement required in the piers. DDBD required less effort than AASHTO LRFD Seismic since pushover analysis was not required. It is also observed that the effort required to obtain an optimum design in AASHTO LRFD Seismic is directly related to the experience of the designed to guess the reinforcement of the sections and avoid iteration.

CONCLUSIONS

- DDBD produces designs in which the bridge meets a predefined level of performance in the critical direction. To obtain a comparable design in AASHTO LRFD Seismic, iteration is needed, varying the amount of reinforcement, until displacement demand equal displacement capacity.
- The application of DDBD requires less effort than the application of AASHTO LRFD Seismic
- DDBD can be applied for any combination of performance and earthquake intensity. Therefore DDBD can be used to meet the performance requirements AASHTO LRFD Seismic, for design in all SDC.

REFERENCES

AASHTO, 2000, *Guide Specifications for Seismic Isolation Design*, 2nd Edition.

AASHTO, 2009, *Guide Specifications for LRFD Seismic Bridge Design*.

Caltrans, 2006, "LRFD Design Example B November 3, 2006," Version 1.1, AASHTO, http://cms.transportation.org/?siteid=34&pageid=1800. (accessed April 18, 2008)

Caltrans, 2008, "Seismic Design Criteria," http://www.dot.ca.gov/hq/esc/techpubs/manual/othermanual/other-engin-manual/seismic-design-criteria/sdc.html. (accessed July 2009)

Calvi, G. M., and Kingsley, G. R., 1995, "Displacement Based Seismic Design of Multi-Degree-of-Freedom Bridge Structures," *Earthquake Engineering and Structural Dynamics*, V. 24, pp. 1247-1266.

Chopra, A., 2000, *Dynamics of Structures: Theory and Applications to Earthquake Engineering*, Prentice Hall.

Dwairi, H., and Kowalsky, M. J., 2006, "Implementation of Inelastic Displacement Patterns in Direct Displacement-Based Design of Continuous Bridge Structures," *Earthquake Spectra*, V. 22, No. 3, pp. 631-662.

EuroCode 8, 1998, "Structures in Seismic Regions—Design: Part 1, General and Building," Commission of European Communities, Report EUR 8849 EN.

FEMA, 2005, "Improvement of Nonlinear Static Seismic Analysis Procedures FEMA440," http://www.fema.gov/library/. (accessed July 2009)

Kowalsky, M. J., 2002, "A Displacement-Based Approach for the Seismic Design of Continuous Concrete Bridges," *Earthquake Engineering and Structural Dynamics*, V. 31, pp. 719-747.

Kowalsky, M. J.; Priestley, M. J. N.; and MacRae, G. A., 1995, "Displacement-Based Design of RC Bridge Columns in Seismic Regions," *Earthquake Engineering and Structural Dynamics*, V. 24, pp. 1623-1643.

Kowalsky, M., and Priestley, N., "Improved Analytical Model for Shear Strength of Circular Reinforced Concrete Columns in Seismic Regions," *ACI Structural Journal*, V. 97, No. 3. May-June 2000

Mander, J. B.; Priestley, M. J. N.; and Park, R., 1988, "Theoretical Stress Strain Model of Confined Concrete," *Journal of Structural Engineering*, ASCE, V. 114, No. 8, Aug.

Ortiz, 2006, "Displacement-Based Design of Continuous Concrete Bridge under Transverse Seismic Excitation," MS thesis, Rose School.

Priestley, M. J. N., 1993, "Myths and Fallacies in Earthquake Engineering-Conflicts between Design and Reality," *Bulletin of the New Zealand Society of Earthquake Engineering*, V. 26, No. 3, pp. 329–341.

Priestley, M. J. N., Calvi, G. M. and Kowalsky, M. J., 2007, *Displacement-Based Seismic Design of Structures*, Pavia, IUSS Press.

Shibata, A., and Sozen, M., "Substitute Structure Method for Seismic Design in R/C," *Journal of the Structural Division,* ASCE, V. 102, No. ST1, 1976, pp. 1-18.

Suarez, V. A., and Kowalsky, M. J., "Displacement-Based Seismic Design of Drilled Shaft Bents with Soil-Structure Interaction," *Journal of Earthquake Engineering*, V. 11, No. 6, Nov. 2007, pp. 1010-1030.

Suarez, V. A., 2008, "Implementation of Direct Displacement Based Design for Highway Bridges," PhD dissertation, North Carolina State University.

Veletsos, A., and Newmark, N. M., 1960, "Effect of Inelastic Behavior on the Response of Simple Systems to Earthquake Motions," *Proceedings of 2nd World Conference on Earthquake Engineering*, pp. 895-912.

SP-271—5

Incorporation of Decoupled Damage Index Models in Performance-Based Evaluation of RC Circular and Square Bridge Columns under Combined Loadings

by A. Belarbi, S. Prakash, and P. F. Silva

Synopsis: This paper investigates the performance-based evaluation of reinforced concrete (RC) bridge circular columns under combined bending, shear, axial, and torsion using decoupled damage index models. The main feature of the proposed damage index model is the feasibility of decoupling these combined actions according to various damage limit states. Research has shown that under combined bending, shear, axial, and torsion loads, the main parameters in the structural performance of RC bridge columns that are affected the most are their strength, deformation capacity, and failure mode. Response of RC columns under these combined actions is very complex and requires the implementation of numerical tools that can quantify the progressive nature of damage under the influence of various parameters. A proper damage index should thus include the main parameters that describe the hysteretic behavior under these combined loadings. Existing damage index models are modified to account for these combined actions in a decoupled scenario which are then used to evaluate the progression of damage under the combined loads.

Under combined loads damage limit states that can be identified are flexural and/or shear/torsion cracking, yielding of transverse and/or longitudinal reinforcement, spalling of concrete cover, and fracture of transverse and longitudinal reinforcement. The main variables that are considered in the study to characterize the damage index are (i) the ratio of torsion-to-bending moment (T/M) for circular columns and twist-to-displacement (q/D) for square columns, (ii) the level of detailing for high and moderate seismicity (low or high transverse reinforcement ratio) and (iii) level of shear (low or moderate). Progression of damage in RC columns due to the interaction between bending and torsion is also evaluated as a function of the transverse reinforcement ratio. Results show that the columns' lateral displacement ductility as well as its torsion rotation ductility are decreased under combined loads. The progression of damage is found to be amplified due to the effects of torsion. An important observation from this study that can have a significant impact in the seismic design of RC columns under combined loads is that an increase in the transverse reinforcement ratio helps delay the progression of damage, thereby changing the response of the columns from a torsional response to a predominately flexural response.

Keywords: circular columns; combined loadings; damage index; performance-based design; square columns; torsion.

Abdeldjelil Belarbi, FACI, is Hugh Roy and Lillie Cranz Cullen Professor and Chairman of the Department of Civil and Environmental Engineering at the University of Houston. His research interests include constitutive modeling of reinforced and prestressed concrete as well as use of advanced materials and smart sensors in civil engineering infrastructure. He is a member of Joint ACI-ASCE Committees 445, Shear and Torsion, and 343, Concrete Bridge Design; and ACI Committees 440, Fiber Reinforced Polymer Reinforcement, and 341, Earthquake-Resistant Concrete Bridges. He is the past Chair of ACI-E801, Student Activities, and current Chair of Subcommittees 445-5, Torsion of Structural Concrete, and 440-E, Professional Education. He is a past President of the ACI Missouri Chapter.

S. Suriya Prakash is a PhD candidate in the department of civil engineering at Missouri University of Science and Technology. His research interests include behavior of RC structural elements and earthquake engineering.

Pedro F. Silva is an Associate Professor at The George Washington University, DC. He is a member of the ACI Committees 440, and 341. His research interests include the development of performance-based procedures for the design and retrofit of structures, and use of fiber reinforcement polymers for the structural rehabilitation of structures.

INTRODUCTION

The main objective of a performance-based design is to combine the complex relationships between the severity of an earthquake and the desired performance of structural components. Since current seismic design codes focus mainly on the strength and serviceability requirements, they do not meet this performance objective. Current design methods are limited; they address designs of structures to meet particular seismic load levels but not necessarily to achieve specific performance objectives that incorporate damage prevention. Such objectives, however, including prescribed damage limit states, can be incorporated into a performance-based design approach.[1,2] Using a performance-based design approach, bridge columns can be designed to meet targeted damage levels and different earthquake motions. For the successful implementation of a performance-based design approach design engineers must use advanced analytical models that incorporate damage evaluation in design in terms of engineering criteria such as strain and ductility levels. To facilitate repair and retrofit decisions, they must also quantify the damage in simple terms under various loading conditions, creating damage indices that take into account various design parameters.

Numerically, performance objectives for structural components under different levels of earthquakes are established from empirically derived hysteresis curves, which incorporate damage indices. Establishment of proper damage indices that take into account the various design parameters is thus an essential step for the successful implementation of a performance-based design approach. Hence, damage indices should be established at prescribed damage limit states that describe the hysteretic behavior under combined loads such as bending, shear, axial, and torsion during earthquakes. There have been numerous studies conducted on development of damage indices based on flexural behavior.[3,4,5,6] Jeong and Elnashai[7] were the first to develop a 3D damage index for reinforced concrete (RC) buildings with planar irregularities, taking into account the bidirectional and torsional response. However, no damage index models have been developed explicitly to study the interaction effects of flexure and torsional damage indices. This study therefore, is the first to define damage indices at various damage limit states for combined loadings.

Existing damage indices for flexural failure mode are extended in this study to combined loadings. This paper has three objectives. First, it presents decoupled damage index models for combined loadings and identifies the implications of combined loadings from the perspective of performance-based seismic design. Second, it reports the trends in progression of damage with respect to an increase in torsion-to-bending moment (T/M) for circular columns tested at Missouri University of Science and Technology (Missouri S&T) and for rotation-to-displacement (θ/Δ) ratio for the square columns tested at University of Tokyo. Effect of increase in the transverse spiral reinforcement ratio and a reduction in shear span is also investigated for circular columns. The progression of damage in square and circular columns are compared and discussed. Finally from a design perspective, it proposes limits on a damage index for various performance levels for circular columns under combined loadings. In order to achieve these objectives, proposed damage index models were validated from test results, and key results are presented here.

COMBINED LOADINGS IN RC BRIDGE COLUMNS

Combined loadings including torsion with axial, shear, and bending occur predominantly in three dimensional structures such as arch ribs, bridge piers, spiral stair cases, bridges with outrigger bents, and spandrel beams. The effect of combined loadings is particularly important in skewed and curved bridges, and in bridges with unequal spans or column heights. Reinforced concrete columns are subjected to combined loadings when structural constraints such as a stiff deck, abutment restraints, and soil conditions are imposed on bridges. The combined loadings results in complex flexural and shear modes of failure in these bridge columns. Location and elongation of the plastic hinge length due to the combination of torsional loading is another adverse effect in RC columns subjected to combined loadings.

The amount of torsional loading increases as the skew of the bridge increases. The strength and stability of bridges are largely dependent on the capacity of RC columns in sustaining inelastic load reversals without experiencing significant decreases in strength when exposed to combined earthquake loadings. Experiments have shown that flexural strength decreases more rapidly with torsional loadings.[8,9,10] Also, it has been found that the transverse reinforcement requirements for confinement of the concrete core may not be adequate in the presence of torsional loadings. Due to eccentricities with respect to the center of mass in curved and skewed bridges, the displacement ductility demand on certain elements may be significantly larger than the ductility demand imposed on the entire system. Therefore, it is necessary to assess rationally the inelastic response of RC columns under combined loadings that result from earthquake motions. Specifically, designers should determine the shear and torsional capacity of columns and predict the damage levels across a wide range of ductility levels (in rotational as well as flexural displacements) so that the structure can be protected against brittle shear failure in the presence of torsional loadings. It is also important to quantify the flexural capacity so that the dependability of flexural hinges can be assessed under dominant shear/torsional loads.

FLEXURAL DISPLACEMENT AND TORSIONAL ROTATION DUCTILITY

Flexural and rotational displacements along the length of a column under combined bending, shear, and torsion are shown in Figure 1. The flexural displacement distribution is essentially linear until yielding of the longitudinal bars on the tension side; thereafter, it becomes nonlinear. The yielding of longitudinal reinforcement and the subsequent crushing of the cover concrete result in the formation of a flexural plastic hinge. Well confined columns tested under bending shear (single curvature) typically form a plastic hinge in the bottom portion where the bending moment is greatest as shown in Figure 1(a). The twist distribution of columns tested under pure torsion is essentially linear until shear cracking, becoming nonlinear thereafter for the full length of the column, as shown in Figure 1(b).

A structural system is said to be ductile if it is capable of undergoing substantial inelastic deformations without loss of strength. Under bending-shear loading, flexural displacement ductility can be derived using the moment curvature relationship and the assumed plastic hinge length. The total flexural displacement of the column under bending-shear can be expressed as the sum of yield displacement and plastic displacement, as shown in Equation 1. Recent works have also improved the estimation of plastic hinge lengths by including the effects of axial load and shear span-to-depth ratio[11].

$$\Delta_t = \Delta_y + \Delta_p = (\phi_u - \phi_y) l_p (L - 0.5 l_p) \tag{1}$$

where Δ_t is the total displacement, Δ_y is the yielding displacement, l_p is the length of the plastic hinge, ϕ_u is the curvature at ultimate moment, and ϕ_y is the curvature at yield moment.

The displacement ductility can be expressed in terms of curvature ductility as shown in Equation 2:

$$\mu_\Delta = 1 + 3(\mu_\phi - 1)\frac{l_p}{L}(1 - 0.5\frac{l_p}{L}) \tag{2}$$

where μ_Δ is the displacement ductility and μ_ϕ is the curvature ductility.

Recent studies have included the effect of axial-flexure-shear interaction in predicting the deformation capacity of RC columns12. However, under combined bending, shear, and torsional loads, the RC columns undergo not only lateral displacement but also lateral twist. Therefore, since they were developed based on bending-shear tests, the above equations are not applicable to columns under combined loadings including torsion.

Rotational ductility under torsion can be defined as the ratio of twist to the corresponding twist at the yielding of the spiral as shown in Equation 3:

$$\mu_\theta = \frac{\theta}{\theta_y} \tag{3}$$

where θ is the twist at the top of the column due to torsional moment, θ_y is the yielding twist at the top of the column due to torsional moment, and μ_θ is the rotational ductility.

Very few studies have examined the behavior of RC columns under combined loadings, and the limited tests on combined loadings pose difficulties in establishing the relationship between curvature and rotational ductility. Further, estimation of flexural displacement using the above equations depends highly on the accuracy of the plastic hinge length calculations.

The interaction between flexural displacement and torsional rotational ductility is complex and little understood due to the paucity of test data. The damage to columns under combined loadings is also complex, affecting either a portion of the column or its whole length. Completely under-reinforced circular columns tested under flexure fail by formation of a plastic hinge in the bottom portion of the column. Completely under-reinforced circular columns tested under pure torsion have shown severe core damage in the middle of the columns although the damage was distributed along the length of the column. If torsion and bending loads are applied to a column simultaneously, the distribution of damage increases depending on the applied torsion-to-bending (*T/M*) ratio as shown in Figure 2.

PREVIOUS RESEARCH ON DAMAGE MODELS

Damage indices provide a means to quantify the damage sustained in concrete structures during earthquakes. Damage indices may be defined locally at the cross section level or at a member level for an individual element or for an entire structure. The earliest and simplest measures of damage were based on displacement ductility, and inter-storey drift. These simple damage indicators, however, consider neither degradation in the stiffness of the member or structure nor energy dissipation under cyclic loads. Current local damage indices are cumulative and depend on damage and the amplitude and number of cycles of loading.[3,5] Damage indices can inform retrofit decisions disaster planning and post-earthquake assessment. They are dimensionless parameters intended to range from lowest value for an undamaged structure to highest value for a structure near or at collapse, with intermediate values estimating the degree of damage. Since these indices are based on flexural behavior, they cannot be used to correlate the limit states corresponding to flexure, shear, and torsion.

Noncumulative damage indices

Damage can be indicated by the ratio of initial stiffness to the secant stiffness corresponding to the maximum displacement in a given cycle as proposed by Banon et al.[13] The authors called their damage index a flexural damage ratio. Later, it was modified[14] to the formulation given by Equation 4, and they defined damage in terms of flexibility.

$$D_{RM} = \frac{f_m - f_0}{f_u - f_0} \tag{4}$$

where D_{RM} = damage index by Raufaiel and Meyer, f_0 = pre-yield flexibility f_m = secant flexibility at a given load and f_u = secant flexibility at ultimate load. However, this formulation does not reliably indicate failure since it does not include the effect of cyclic loading.

Energy-based cumulative damage indices

Park and Ang damage index—This is a linear combination of non cumulative and cumulative damage index.[15] The Park and Ang model is defined in terms of Equation 5 in which the first term accounts for ductility in the system and the second term is related to the normalized cumulative energy absorbed by the member.